J|A|C|S
COMMUNICATIONS

Published on Web 09/30/2004

A Theoretical Investigation of Ruthenium-Catalyzed Alkene Hydrosilation: Evidence To Support an Exciting New Mechanistic Proposal

Chad Beddie and Michael B. Hall*

Department of Chemistry, Texas A&M University, College Station, Texas 77843-3255

Received June 11, 2004; E-mail: hall@science.tamu.edu

Hydrosilation is a key catalytic reaction for the production of industrially important organosilicon products, and consequently, hydrosilation reactions have been studied extensively.[1] Recently, Tilley and co-workers developed a cationic ruthenium silylene catalyst system capable of facilitating highly regioselective anti-Markovnikov hydrosilation of alkenes.[2] To account for the unusual properties of the ruthenium catalyst system, Tilley and co-workers proposed a novel mechanism in which the key step is alkene insertion into a *silicon−hydrogen* bond located in a position *remote* from the metal center (Scheme 1). This mechanism is unlike any other proposed for late transition metal-catalyzed hydrosilation, since in all other commonly accepted proposals, bond formation occurs via coordination of both silane and olefin to the transition metal.[3] Since the identification of a new hydrosilation mechanism has important ramifications for the design of new hydrosilation catalysts and, more generally, potential applicability for the design of new catalytic processes,[4] the catalytic hydrosilation of alkenes by cationic ruthenium silylene complexes was investigated using density functional theory methods.[5,6] These investigations indicate that the mechanism proposed by Tilley and co-workers is favored by more than 8 kcal/mol relative to Chalk−Harrod and modified Chalk−Harrod mechanisms.

Scheme 1. Catalytic Hydrosilation Cycle Involving Ethylene Insertion into a Remote Silicon Hydrogen Bond[a]

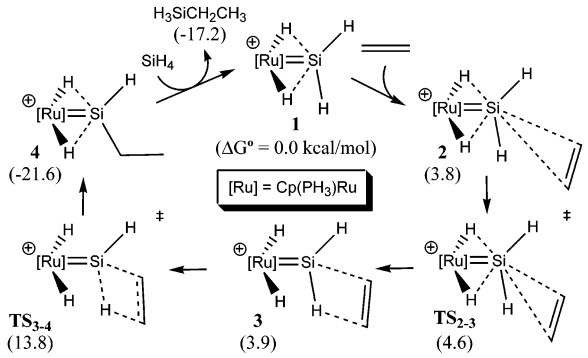

[a] Relative free energies of the intermediates ($\Delta G°$) and transition states ($\Delta G^{‡}$) are provided in parentheses in kcal/mol.

The catalytic cycle involving ethylene insertion into a Si−H bond remote from the ruthenium center is presented in Scheme 1. The cationic silylene complex $[Cp(PH_3)Ru(H)_2(SiH_2)]^+$ **1** represents the starting point of the model catalytic cycle. **1** is generated via the release of OMe_2 from $[Cp(PH_3)Ru(H)_2(SiH_2)\text{-}OMe_2]^+$.[7] In the gas phase, OMe_2 strongly coordinates to silicon, and therefore release of OMe_2 is disfavored by 13.0 kcal/mol.[8] However, incorporation of solvent effects reduces the endoergicity of this process to 8.6 kcal/mol.[9] Coordination of ethylene to **1** affords an ethylene π-complex, **2**, in which the C−Si distances are 3.04 and 3.02 Å, respectively. In **2**, the Si−Ru distance is 2.30 Å, while the distances from Si to the bridging Ru−H's are 1.68 and 1.72 Å, respectively. The $Ru(H)_2(SiH_2)$ core of **2** has a very similar structure to **1**, in which the corresponding distances are 2.34, 1.62, and 1.62 Å, respectively. Both **1** and **2** have character reminiscent of silane interacting with ruthenium through two Si−H σ-complex interactions. A transition-state structure from **1** to **2** was not calculated since this barrier is expected to be negligible because of the small structural changes that are observed.

Progressing from **2** through $\mathbf{TS_{2-3}}$ yields another ethylene π-complex, **3**. In **3**, the ethylene is much closer to the silicon, with C−Si bond distances of 2.44 and 2.53 Å, respectively. The closer proximity of the ethylene to the silicon weakens the interaction with the bridging Ru−H's, as indicated by an increase in the observed distances (2.33 and 1.98 Å, respectively). Despite the structural changes, **2** and **3** are very similar in energy. The barrier to interconversion between **2** and **3** is less than 1 kcal/mol.

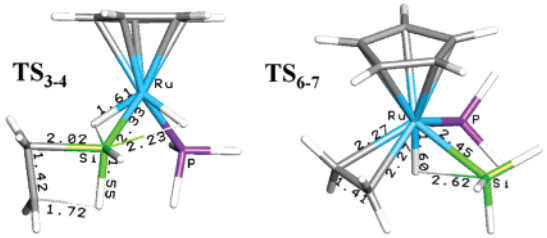

Figure 1. JIMP representations of $\mathbf{TS_{3-4}}$, the transition state for ethylene insertion into the Si−H bond that represents the highest energy structure in the mechanism proposed by Tilley, and $\mathbf{TS_{6-7}}$, the transition state for Si−H oxidative addtion that represents the highest energy structure along the lowest energy Chalk−Harrod and modified Chalk−Harrod pathways.

The next step in this pathway is conversion of **3** to the coordinated hydrosilation product **4** via insertion of ethylene into the Si−H bond. The transition state for this process, $\mathbf{TS_{3-4}}$, is shown in Figure 1. In $\mathbf{TS_{3-4}}$, the C−Si bond has nearly formed, as indicated by a C−Si distance of 2.02 Å. In contrast, the future C−H bond is quite long in $\mathbf{TS_{3-4}}$, while the Si−H distance has only lengthened slightly relative to the Si−H distance in **3**. The vibrational motion of imaginary frequency represents the breaking of the Si−H bond and formation of the C−H bond. The relative free energy of this transition state, $\mathbf{TS_{3-4}}$, is only 13.8 kcal/mol; therefore, ethylene insertion into the silicon−hydrogen bond is an extremely viable process. The catalytic cycle is completed via the stepwise displacement of $H_3SiCH_2CH_3$ from **4** by SiH_4 to regenerate **1**.[10] The highest energy transition state in this process, $\mathbf{TS_{S4-S5}}$, has a relative energy of −2.7 kcal/mol, more than 19 kcal/mol higher in energy than **4**; thus, $H_3SiCH_2CH_3$ release represents the rate-determining step of the catalytic cycle in Scheme 1.

Unlike the low barrier to C−Si bond formation for the new mechanism proposed by Tilley and co-workers, the barriers to C−Si bond formation for all of the calculated Chalk−Harrod and modified Chalk−Harrod mechanisms were quite high, as the highest energy transition states in these pathways exhibit free energies of at least 22.4 kcal/mol relative to separated ethylene and **1** (Scheme 2).

10.1021/ja046525z CCC: $27.50

Scheme 2. Lowest Energy Chalk−Harrod and Modified Chalk−Harrod Mechanisms[a]

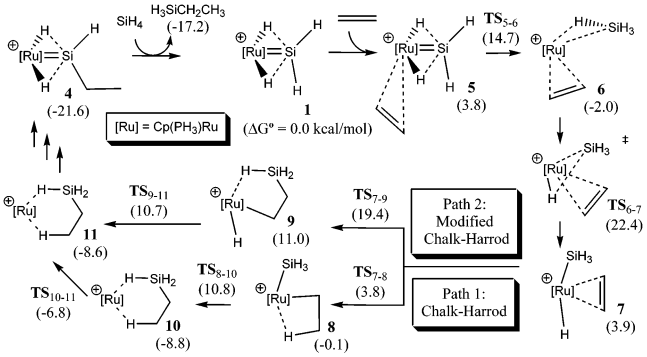

[a] Relative free energies of the intermediates ($\Delta G°$) and transition states ($\Delta G^{‡}$) are provided in parentheses in kcal/mol.

The lowest energy Chalk−Harrod and modified Chalk−Harrod mechanisms are illustrated in Scheme 2.[11] Both mechanisms begin from **1**. Ethylene weakly interacts with **1** to generate **5**, in which the ethylene C−Ru distances are 5.76 and 6.10 Å, respectively. Ethylene coordinates tightly to ruthenium through $\mathbf{TS_{5-6}}$ (14.7 kcal/mol) to form **6** (−2.0 kcal/mol), in which SiH_4 is coordinated to ruthenium via a σ-complex interaction. From **6**, the rate-determining step for both pathways is oxidative addition of SiH_4 via $\mathbf{TS_{6-7}}$ (22.4 kcal/mol, Figure 1) to form intermediate **7**. From **7**, the Chalk−Harrod and modified Chalk−Harrod pathways diverge. In the Chalk−Harrod pathway (Path 1, Scheme 2), C−H bond formation occurs first, as **7** is converted to **8** via $\mathbf{TS_{7-8}}$. The energy barrier for this process is negligible. From **8**, C−Si bond formation occurs through $\mathbf{TS_{8-10}}$ (10.8 kcal/mol) to form the ruthenium hydrosilation-product adduct **10**. A slight structural rearrangement of **10** via $\mathbf{TS_{10-11}}$ yields **11**. In the modified Chalk−Harrod mechanism (Path 2, Scheme 2), C−Si bond formation occurs from **7**, via $\mathbf{TS_{7-9}}$ (19.4 kcal/mol), to form **9**. Subsequently, C−H bond formation occurs via reductive elimination with a negligible barrier through $\mathbf{TS_{9-11}}$ to form **11**. The catalytic cycles for both mechanisms are completed by isomerization of **11** to **4** through a series of low barrier rotations,[12] followed by stepwise displacement of $H_3SiCH_2CH_3$ from **4** by SiH_4 to regenerate **1**.[10]

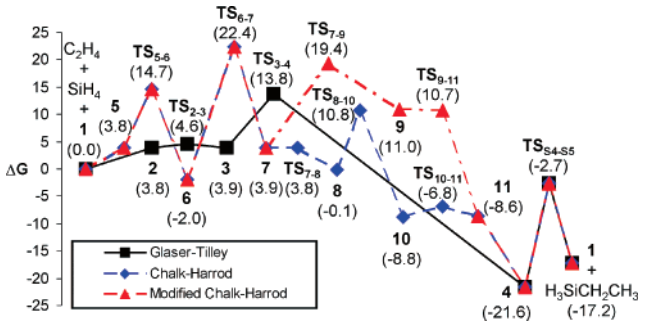

Figure 2. Relative free energies (kcal/mol) of the intermediates ($\Delta G°$) and transition states ($\Delta G^{‡}$) for the hydrosilation mechanisms illustrated in Schemes 1 and 2. For simplicity, the multistep pathway from **11** to **4** has been illustrated as a single line, whereas the multistep pathway from **4** to **1** is represented as a single transition state, $\mathbf{TS_{S4-S5}}$, the highest energy transition state in the displacement of $H_3SiCH_2CH_3$ by SiH_4.

Figure 2 clearly demonstrates that the Glaser−Tilley mechanism provides the lowest energy hydrosilation pathway from **1**. However, in the event ethylene does coordinate to ruthenium to form **6**, it should be noted that it is more energetically favorable for ethylene to dissociate from the ruthenium center via $\mathbf{TS_{5-6}}$ (14.7 kcal/mol) to form **5** than to proceed forward through the Chalk−Harrod and modified Chalk−Harrod mechanisms. From **5**, ethylene is free to dissociate to form **1**, then coordinates to form **2** and proceeds to the hydrosilation product via the lower energy pathway proffered by the Glaser−Tilley mechanism (Figure 2).

In conclusion, this study provides the first theoretical evidence for an important new hydrosilation mechanism. The highest energy transition state in the novel hydrosilation mechanism proposed by Tilley and co-workers is more than 8 kcal/mol lower in energy than the highest energy transition states in Chalk−Harrod and modified Chalk−Harrod mechanisms. Preliminary investigations using more realistic model ligands support the conclusion that the Glaser−Tilley mechanism is the lowest-energy pathway, although the differences in energy are smaller. These results will be discussed in detail in subsequent reports.

Acknowledgment. We thank the NSF (CHE 98-00184, MRI 02-16275) and the Welch Foundation (A-0648) for support.

Supporting Information Available: Details of calculations and schematic representations of alternative catalytic pathways. This material is available free of charge via the Internet at http://pubs.acs.org.

References

(1) (a) Tilley, T. D. In *The Chemistry of Organic Silicon Compounds*; Patai, S., Rappoport, Z., Eds.; Wiley & Sons: New York, 1989; pp 1415−1477. (b) Ojima, I. In *The Chemistry of Organic Silicon Compounds*; Patai, S., Rappoport, Z., Eds.; Wiley & Sons: New York, 1989; pp 1479−1526. (c) Marciniec, B. *Appl. Organomet. Chem.* **2000**, *14*, 527−538 and references therein.
(2) Glaser, P. B.; Tilley, T. D. *J. Am. Chem. Soc.* **2003**, *125*, 13640−13641.
(3) For example, in the Chalk−Harrod mechanism, olefin inserts into the metal−hydrogen bond: (a) Chalk, A. J.; Harrod, J. F. *J. Am. Chem. Soc.* **1965**, *87*, 16−21. (b) Chalk, A. J.; Harrod, J. F. *J. Am. Chem. Soc.* **1965**, *87*, 1133−1135. In the modified Chalk−Harrod mechanism proposed by Sietz and Wrighton, olefin inserts into the metal-silicon bond: (c) Seitz, F.; Wrighton, M. S. *Angew. Chem., Int. Ed. Engl.* **1988**, *27*, 289−291. (d) Duckett, S. B.; Perutz, R. N. *Organometallics* **1992**, *11*, 90−98. Furthermore, σ-bond metathesis hydrosilation mechanisms that are proposed for d^0 metals also occur within the first coordination sphere of the transition metal: (e) Corey, J. Y.; Zhu, X.-H. *Organometallics* **1992**, *11*, 672−683. (f) Kesti, M. R.; Waymouth, R. M. *Organometallics* **1992**, *11*, 1095−1103.
(4) Brunner, H. *Angew. Chem., Int. Ed.* **2004**, *43*, 2749−2750.
(5) For theoretical investigations on other hydrosilation catalysts, see: (a) Sakaki, S.; Takayama, T.; Sumimoto, M.; Sugimoto, M. *J. Am. Chem. Soc.* **2004**, *126*, 3332−3348. (b) Chung, L. A.; Wu, Y.; Trost, B. M.; Ball, Z. T. *J. Am. Chem. Soc.* **2003**, *125*, 11578−11582. (c) Sakaki, S.; Sumimoto, M.; Fukuhara, M.; Sugimoto, M.; Fujimoto, H.; Matsuzaki, S. *Organometallics* **2002**, *21*, 3788−3802 and references therein.
(6) All calculations were conducted using the Gaussian03 suite of programs: Frisch, M. J.; Trucks, G. W.; Schlegel, H. B.; Scuseria, G. E.; Robb, M. A.; Cheeseman, J. R.; Montgomery, J. A., Jr.; Vreven, T.; Kudin, K. N.; Burant, J. C.; Millam, J. M.; Iyengar, S. S.; Tomasi, J.; Barone, V.; Mennucci, B.; Cossi, M.; Scalmani, G.; Rega, N.; Petersson, G. A.; Nakatsuji, H.; Hada, M.; Ehara, M.; Toyota, K.; Fukuda, R.; Hasegawa, J.; Ishida, M.; Nakajima, T.; Honda, Y.; Kitao, O.; Nakai, H.; Klene, M.; Li, X.; Knox, J. E.; Hratchian, H. P.; Cross, J. B.; Adamo, C.; Jaramillo, J.; Gomperts, R.; Stratmann, R. E.; Yazyev, O.; Austin, A. J.; Cammi, R.; Pomelli, C.; Ochterski, J. W.; Ayala, P. Y.; Morokuma, K.; Voth, G. A.; Salvador, P.; Dannenberg, J. J.; Zakrzewski, V. G.; Dapprich, S.; Daniels, A. D.; Strain, M. C.; Farkas, O.; Malick, D. K.; Rabuck, A. D.; Raghavachari, K.; Foresman, J. B.; Ortiz, J. V.; Cui, Q.; Baboul, A. G.; Clifford, S.; Cioslowski, J.; Stefanov, B. B.; Liu, G.; Liashenko, A.; Piskorz, P.; Komaromi, I.; Martin, R. L.; Fox, D. J.; Keith, T.; Al-Laham, M. A.; Peng, C. Y.; Nanayakkara, A.; Challacombe, M.; Gill, P. M. W.; Johnson, B.; Chen, W.; Wong, M. W.; Gonzalez, C.; Pople, J. A. *Gaussian 03*, revision B.4; Gaussian, Inc.: Pittsburgh, PA, 2003.
(7) In this computational investigation, the experimental cation, $[Cp^*(P(i\text{-}Pr)_3\text{-}Ru(H)_2(SiH_2)\text{-}OEt_2]^+$, and the experimental substrate, $PhSiH_3$, were modeled using $[Cp(PH_3)RuH_2(SiH_2)\text{-}OMe_2]^+$ and SiH_4, respectively, to save computational time.
(8) All relative free energies were calculated in the gas phase with complex **1** and separated ethylene set to 0.0 kcal/mol unless otherwise noted.
(9) CPCM calculations employing dichloromethane as a solvent. See the Supporting Information for more details.
(10) See Scheme S2 in the Supporting Information for more details.
(11) Separate Chalk−Harrod and modified Chalk−Harrod mechanisms that involve σ-bond metathesis steps that couple C−H and C−Si bond formation with Si−H oxidation were also identified; these pathways demonstrated even higher overall barriers to hydrosilation and are illustrated in the Supporting Information.
(12) See Scheme S9 in the Supporting Information for more details.

JA046525Z